2016

Domain wall conductivity in semiconducting hexagonal ferroelectric $TbMnO_3$ thin films

D. J. Kim
University of Nebraska - Lincoln

J. G. Connell
University of Kentucky

S. S. A. Seo
University of Kentucky

Alexei Gruverman
University of Nebraska-Lincoln, agruverman2@unl.edu

IOP Publishing Nanotechnology
Nanotechnology 27 (2016) 155705 (6pp) doi:10.1088/0957-4484/27/15/155705

Domain wall conductivity in semiconducting hexagonal ferroelectric $TbMnO_3$ thin films

D J Kim[1,2,3], J G Connell[4], S S A Seo[4] and A Gruverman[1]

[1] Department of Physics and Astronomy, University of Nebraska-Lincoln, Lincoln, NE 68588, USA
[2] Center for Correlated Electron Systems, Institute for Basic Science, Seoul 151-742, Korea
[3] Department of Physics and Astronomy, Seoul National University, Seoul 151-742, Korea
[4] Department of Physics and Astronomy, University of Kentucky, Lexington, KY 40506, USA

E-mail: djkim5150@gmail.com and agruverman2@unl.edu

Received 9 January 2016
Accepted for publication 9 February 2016
Published 2 March 2016

Abstract

Although enhanced conductivity of ferroelectric domain boundaries has been found in $BiFeO_3$ and $Pb(Zr,Ti)O_3$ films as well as hexagonal rare-earth manganite single crystals, the mechanism of the domain wall conductivity is still under debate. Using conductive atomic force microscopy, we observe enhanced conductance at the electrically-neutral domain walls in semiconducting hexagonal ferroelectric $TbMnO_3$ thin films where the structure and polarization direction are strongly constrained along the *c*-axis. This result indicates that domain wall conductivity in ferroelectric rare-earth manganites is not limited to charged domain walls. We show that the observed conductivity in the $TbMnO_3$ films is governed by a single conduction mechanism, namely, the back-to-back Schottky diodes tuned by the segregation of defects.

Keywords: hexagonal manganite, domain wall conductivity, semiconducting, ferroelectric, conductive atomic force microscopy, back-to-back Schottky barrier

(Some figures may appear in colour only in the online journal)

1. Introduction

In the field of oxide and semiconductor electronics, attention has been shifting from bulk materials to the interfaces [1]. This shift is a result of an observation of a number of important and interesting phenomena, such as a two-dimensional electron gas [2] and a memristive switching behavior [3, 4] associated with the interface properties. The active interfaces termed heterointerfaces are defined by the fabrication of structures from different materials. Generally, such heterostructures are difficult to fabricate because they require coherent growth [1, 2].

At the same time, homointerfaces such as ferroic domain walls started to attract attention, because of their intrinsic coherence, nanometer thickness, mobility, and rich physics [5–7]. Domain walls are archetypal homointerfaces between regions which have different orientations of an order parameter within an ordered ferroic material. It has been reported that domain walls exhibit intriguing properties [6] for example, a finite magnetization in a multiferroic [8] and enhanced/decreased conductivity in ferroelectrics [9–13]. Among them, conductive domain walls in ferroelectrics have great potential to overcome the limitations of conventional electronics by endowing electronic devices with a resistive tunability.

Since the first report of domain walls conduction in multiferroic $BiFeO_3$ thin films [9], intense studies of this effect in other ferroelectrics have been carried out [10–16]. Recent observations of enhanced/reduced conductance at domain walls in $Pb(Zr,Ti)O_3$ films [17], $LiNbO_3$ [18] and hexagonal rare-earth manganite (*h*-*Re*MnO_3) single crystals [14–16] suggest that the domain wall conductivity is universal in ferroelectrics. In particular, the domain wall conductivity in *improper* ferroelectric *h*-*Re*MnO_3 should be more intriguing thanks to the presence of energetically unfavorable charged domain walls stabilized by the interlocking of structural phase boundaries and domain walls, and the presence of topological defects and vortices [19]. The recently reported conductivity at domain walls in *h*-$HoMnO_3$ and *h*-$ErMnO_3$ can be understood as a consequence of changes in the band structure at the domain walls and accumulation of the charge carriers compensating the charged domain walls [14, 15]. However, investigation of domain wall conductivity in *h*-*Re*MnO_3 has

thus far been focused on single crystals, while there has been no studies on thin films. Here, we report enhanced domain wall conductivity in ferroelectric *h*-$TbMnO_3$ thin films [20] epitaxially stabilized on Pt/Al_2O_3 substrates [21].

2. Sample fabrication and methods

Epitaxial *h*-$TbMnO_3$ thin films are grown on Pt(111)/Al_2O_3(0001) substrates using a pulsed laser deposition (PLD) system equipped with *in situ* reflection high-energy electron diffraction (RHEED) and optical spectroscopic ellipsometry (SE) [22]. Prior to deposition of the *h*-$TbMnO_3$ film, a Pt bottom layer is deposited on a (0001) Al_2O_3 single crystal substrate at 600 °C using rf-sputtering. The optimal growth conditions of *h*-$TbMnO_3$ thin films in PLD are found to be the following: a substrate temperature of 800 °C, an oxygen partial pressure of 30 mTorr, and a KrF excimer ($\lambda = 248$ nm) laser fluence of 1.2 J cm^{-2}. The coherent growth of hexagonal $TbMnO_3$ film is confirmed by RHEED and SE monitoring during deposition. The thickness of the deposited *h*-$TbMnO_3$ film is ~23 nm. X-ray diffraction scans reveal the hexagonal structure of the grown epitaxial films [20]. Atomic force microscopy (MFP-3D, Asylum Research) is used to acquire local conductance maps and current–voltage (*I*–*V*) curves at different locations with an electrically biased conductive diamond-coated tip (Nanosensors). Bias for writing a resistance state or reading a current is applied to the bottom electrode while the tip is grounded.

3. Results

In our previous work [20], room-temperature ferroelectricity and polarization-dependent resistive switching in *h*-$TbMnO_3$ thin films with the spontaneous polarization constrained to the film normal direction by strain have been reported. The subsequent observations of a local conductance reveal the enhanced domain wall conductivity of ferroelectric *h*-$TbMnO_3$ thin films. To align the polarization, the write voltage of ±6 V, which is large enough compared to the coercive voltage of around ±3 V, is applied to the bottom electrode. In figure 1(a), the difference in conductance between negatively (OFF; $-6\ V_{write}$) and positively (ON; $6\ V_{write}$) poled areas at the 0.5 V read-bias, is barely visible. There are mesas of a low resistance, which are not identified but believed to be structural/vacancy defects or different phases other than *h*-$TbMnO_3$. With an increased read-bias in the range of 1.0–1.5 V, conduction of the boundary between the OFF and surrounding unpoled regions (OFF/unpoled boundary) becomes visible (figures 1(b) and (c)). Only the conduction at the OFF/unpoled boundary is visible, while the conduction at the boundary between the OFF and the ON regions (OFF/ON boundary) is not, because the strong conduction of the ON region conceals the conduction of the OFF/ON boundary. With a higher read-bias (2.0 V, figure 1(d)), the conduction of the OFF/unpoled boundary is not seen any longer because it becomes indistinguishable from the increased conduction of the surrounding unpoled region. There is no modification of the topography and the current map by repeated scanning, which indicates that the conductance change is not due to surface damage by the tip and that the reading voltage does not affect the conductance state of the scanned area.

The conduction of the OFF/unpoled boundary is not uniform, as well as the conduction within the ON and unpoled regions. Figures 2(a) and (b) show a histogram analysis of the current distribution within the ON and OFF regions, the unpoled region and the OFF/unpoled boundary, acquired from figure 1(c). Each distribution is well fitted by a log-normal function, except for the OFF region, which is too narrow to fit. A lognormal distribution of current implies a Gaussian distribution of the conduction barrier properties, namely effective barrier thickness and height [23, 24]. Given that the surface roughness does not have sufficient spatial variation to produce a broad lognormal distribution (the root-mean-square roughness of the surface, from which the data of figure 2 have been taken, is less than 0.5 nm, while the film thickness is ~23 nm), it is expected that the observed conduction through the film is governed mainly by the effective conduction barrier height, not by the barrier thickness. From the distribution and the averaged current values, as shown in figure 2(c), we find that the overall resistances of the states, $R_{OFF} > R_{unpoled} > R_{OnBoundary} > R_{ON}$.

Figures 3(a)–(d) show the *I*–*V* curves measured at several randomly chosen locations in the ON and OFF regions, the unpoled region, and at the OFF/unpoled boundary. In spite of the fluctuations, it is clearly seen that the current at the OFF/unpoled boundary (figure 3(b)) is larger than the current in the OFF and unpoled regions. Regarding the *I*–*V* characteristics, the conduction mechanism through the film is not obviously a quantum mechanical tunneling since the film is too thick (~23 nm). Given that *h*-$TbMnO_3$ is a narrow band gap semiconductor with a 1.4 eV band gap [25], a model of back-to-back Schottky barriers can be invoked to explain the observed *I*–*V* curves [20]. This model has two fitting parameters, the Schottky barrier height and the ideality factor of the interfaces. The ideality factor reflects non-ideal effects such as interface states, image-forces, etc. Unfortunately, due to a lack of physical information such as the effective contact area between the tip and the film surface and due to a strong spatial inhomogeneity of the *I*–*V* characteristics, it is not possible to extract meaningful barrier height values from *I*–*V* curve fitting within this model. However, as reported earlier [20] and as seen in figure 3(e), all *I*–*V* curves in figures 3(a)–(d), once normalized by their values at 2.5 V, can be well described by a single universal fitting curve of the back-to-back Schottky barriers model [26]. This means that the ideality factor of all the *I*–*V* curves in figure 3 can be specified as a universal value while one can obtain qualitative information of the Schottky barrier height [20]. To summarize, the conduction observed in the ON and OFF regions, the unpoled region, and at the OFF/unpoled boundary has the universal ideality factor of 1.09 and the barrier height is the sole parameter governing the resistance state. From the averaged current values in figure 2(c), the differences between the

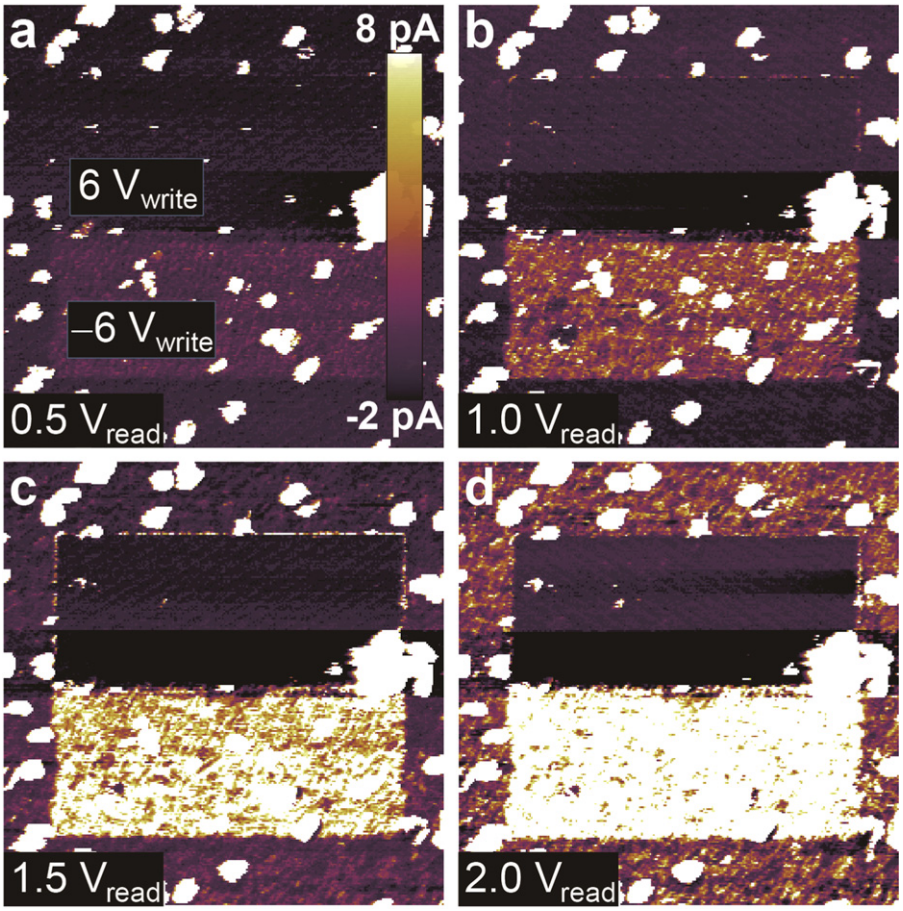

Figure 1. Local current images of hexagonal $TbMnO_3$ film obtained with (a) 0.5 V, (b) 1.0 V, (c) 1.5 V, and (d) 2.0 V biased tip. Positively poled areas (6 V; upper) show a high resistance state while negatively poled areas (−6 V; lower) show a low resistance state. The scan size is $6 \times 6\ \mu m^2$.

barrier heights are roughly 0.17 eV (ON versus OFF), 0.15 eV (on Boundary versus OFF) and 0.13 eV (Unpoled versus OFF).

4. Discussion

We have observed the inhomogeneous enhanced conductance at the OFF/unpoled boundary between the unpoled region and the positively poled (OFF) region. It is necessary to identify a domain structure at the OFF/unpoled boundary. The unpoled region is believed to be associated with a polydomain structure of up and down polarization. Piezoresponse force microscopy (PFM) does not allow one to visualize it due to the small domain size, which is below the PFM resolution limit. Accordingly, the domain structure at the OFF/unpoled boundary should be a combination of up/up and up/down polarization configurations. Here, the up/up polarization configuration is relevant neither to a domain wall nor to the enhanced conduction at the boundary since the up domain has a high resistance (the OFF region).

Thus, at the OFF/unpoled boundary, the enhanced conduction can be attributed to the 180° domain wall itself. However, the exact mechanism of conductivity at ferroelectric domain walls is still under debate [6, 7, 17–19]. So far, several possible mechanisms have been proposed: (1) an electrostatic potential step due to the discontinuity of in-plane polarization at the domain wall [9, 10]; (2) a lowering of the band gap due to structural changes across the domain wall [9]; and (3) a strain-associated segregation of oxygen vacancies at the domain wall, resulting in a lowering of the Schottky barrier [13]. The first explanation cannot be applied in our case because the polarization in our sample has no in-plane component and, therefore, the polarization component normal to the wall should be zero. The neutral 180° domain walls in an epitaxial $Pb(Zr,Ti)O_3$ film may have some charged portion by forming a flux-closure domain formation [17], given the direct observation of continuous polarization rotation at the domain wall with transmission electron microscopy (TEM) [27]. However, in our *h*-$TbMnO_3$ films, as the domain walls and the structural antiphase boundaries in *h*-*Re*MnO_3 are interlocked tightly [19, 28], a continuous rotation of polarization producing a charged domain wall is not likely. It would be of interest to investigate the local domain configurations at the domain walls in this material by high-resolution TEM.

One can assume that a structural change at the structural antiphase boundary (interlocked with a domain wall) may

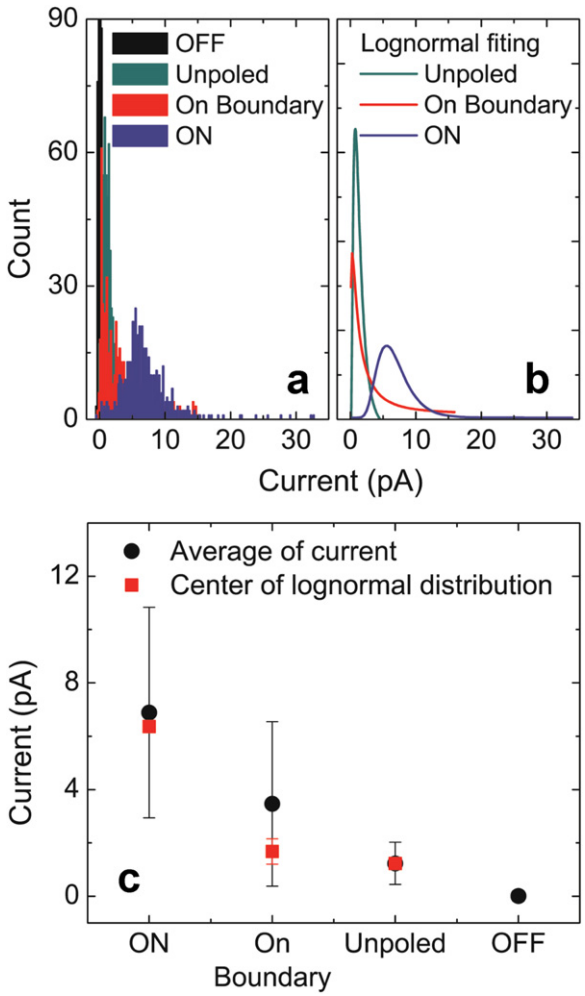

Figure 2. (a) Distribution of current acquired on high (OFF) and low (ON) resistance areas, at an OFF/unpoled boundary, and on an unpoled as-grown area with 1.5 V read bias and (b) every distribution is well described by a lognormal function except for OFF due to that distribution being too narrow. (c) Averaged values of the current and center values of the fitted lognormal functions acquired on the OFF and ON areas, at the boundary, and on the as-grown unpoled region, respectively. Error bars indicate standard deviation of current and width of the distributions.

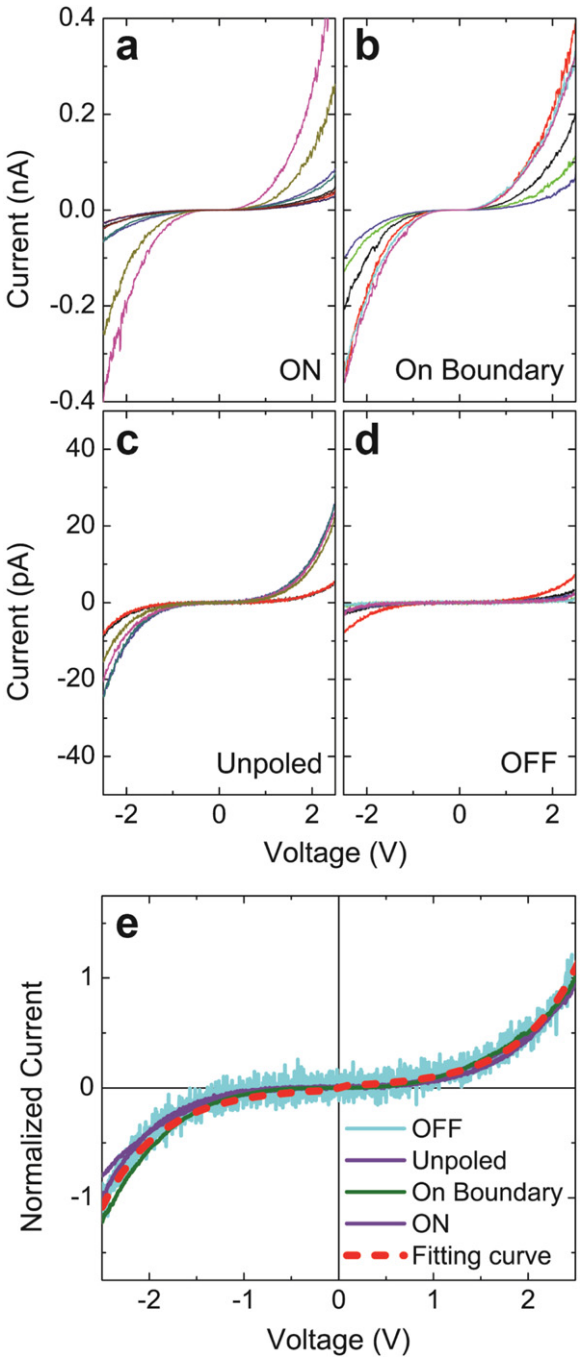

Figure 3. *I–V* curves measured at many spots in (a) the ON region, (b) at the OFF/unpoled boundary, (c) in the unpoled region, and (d) in the OFF region of a hexagonal $TbMnO_3$ film. (e) *I–V* curves normalized by their values at 2.5 V of (a) ~ (d). The red dashed line is a fitting result using the back-to-back Schottky barrier model with an ideality factor of 1.09 and an arbitrary barrier height. The normalized *I–V* curves of OFF, unpoled, and ON and the fitting curve are reproduced from [20]. Copyright WILEY.

reduce the band gap [6, 9, 14], providing a conduction path. However, recent first-principle calculations showed that the local band gap does not change at the neutral domain walls in *h*-$YMnO_3$ [28], so the possibility of band gap modification at the structural antiphase boundary can be ruled out. The accumulation of oxygen vacancies at the domain walls [12, 13], which results in a reduced Schottky barrier and a conduction path [29], is thus the most probable mechanism of the domain wall conduction in the *h*-$TbMnO_3$ film. The oxygen vacancies can be considered as mobile positive charges, able to migrate to thermodynamically stable positions under applied electric field. When a domain is written, a biased tip sweeps away oxygen vacancies inside the film, which are accumulated at the structural antiphase boundary. This scenario is consistent with the random distribution of effective conduction barriers at the domain walls. Moreover, the fact that the domain wall conduction evidently can be tuned by the density of oxygen vacancies in an *h*-$YMnO_3$ single crystal [14] supports the assumption that oxygen vacancies play the most important role in the domain wall conduction of *h*-*Re*MnO_3. There is also no contradiction between this scenario and the back-to-back Schottky barrier

model. Thus, we attribute the conduction of the OFF/unpoled boundary to the domain wall conduction associated with charged defects such as oxygen vacancies in our semiconducting hexagonal ferroelectric $TbMnO_3$ thin film.

5. Conclusion

In summary, we have investigated the domain wall conductivity in ferroelectric hexagonal $TbMnO_3$ thin films using conductive atomic force microscopy. Besides charged domain wall conductivity in *h-Re*MnO_3 films and single crystals, neutral domain walls of hexagonal $TbMnO_3$ film show enhanced conductivity, indicating the domain wall conductivity to be a universal property. Although further investigations are required to confirm the details of the domain wall conductivity of the hexagonal $TbMnO_3$ film, a pure electrostatic/electronic effect in association with defect chemistry based on the back-to-back Schottky diodes structure should be considered.

Acknowledgments

Research at the University of Nebraska–Lincoln was supported by the US Department of Energy, Materials Sciences Division, under Award No. DE-SC0004876 (conductive atomic force microscopy characterization) and the National Science Foundation (NSF) through the Nebraska Materials Research Science and Engineering Center (MRSEC) under Grant No. DMR-1420645 (modeling). The work (sample preparation) at the University of Kentucky was supported by the NSF through Grant No. DMR-1454200, No. EPS-0814194 (the Center for Advanced Materials), and by the Kentucky Science and Engineering Foundation with the Kentucky Science and Technology Corporation through Grant Agreement No. KSEF-148-502-14-328. DJK was partly supported by IBS-R009-G1.

References

[1] Mannhart J and Schlom D G 2010 Oxide interfaces—an opportunity for electronics *Science* **327** 1607
[2] Ohtomo A and Hwang H Y 2004 A high-mobility electron gas at the $LaAlO_3/SrTiO_3$ heterointerface *Nature* **427** 423
[3] Yang J J, Pickett M D, Li X, Ohlberg D A A, Stewart D R and Williams R S 2008 Memristive switching mechanism for metal/oxide/metal nanodevices *Nat. Nanotechnol.* **3** 429
[4] Kim D J, Lu H, Ryu S, Bark C-W, Eom C-B, Tsymbal E Y and Gruverman A 2012 *Nano Lett.* **12** 5697
[5] Allwood D A, Xiong G, Faulkner C C, Atkinson D, Petit D and Cowburn R P 2005 Magnetic domain-wall logic *Science* **309** 1688
[6] Catalan G, Seidel J, Ramesh R and Scott J F 2012 Domain wall nanoelectronics *Rev. Mod. Phys.* **84** 119
[7] Vasudevan R K, Wu W, Guest J R, Baddorf A P, Morozovska A N, Eliseev E A, Balke N, Nagarajan V, Maksymovych P and Kalinin S V 2013 Domain wall conduction and polarization-mediated transport in ferroelectrics *Adv. Funct. Mater.* **23** 2592
[8] Přívratská J 2007 Possible appearance of spontaneous polarization and/or magnetization in domain walls associated with non-magnetic and non-ferroelectric domain pairs *Ferroelectrics* **353** 116
[9] Seidel J *et al* 2009 Conduction at domain walls in oxide multiferroics *Nat. Mater.* **8** 229
[10] Lubk A, Gemming S and Spaldin N A 2009 First-principles study of ferroelectric domain walls in multiferroic bismuth ferrite *Phys. Rev.* B **80** 104110
[11] Seidel J *et al* 2010 Domain wall conductivity in La-doped $BiFeO_3$ *Phys. Rev. Lett.* **105** 197603
[12] Maksymovych P, Seidel J, Chu Y H, Wu P, Baddorf A P, Chen L-Q, Kalinin S V and Ramesh R 2011 Dynamic conductivity of ferroelectric domain walls in $BiFeO_3$ *Nano Lett.* **11** 1906
[13] Farokhipoor S and Noheda B 2011 Conduction through 71° domain walls in $BiFeO_3$ thin films *Phys. Rev. Lett.* **107** 127601
[14] Du Y, Wang X L, Chen D P, Dou S X, Cheng Z X, Higgins M, Wallace G and Wang J Y 2011 Domain wall conductivity in oxygen deficient multiferroic $YMnO_3$ single crystals *Appl. Phys. Lett.* **99** 252107
[15] Wu W, Horibe Y, Lee H, Cheong S-W and Guest J R 2012 Conduction of topologically protected charged ferroelectric domain walls *Phys. Rev. Lett.* **108** 077203
[16] Meier D, Seidel J, Cano A, Delaney K, Kumagai Y, Mostovoy M, Spaldin N A, Ramesh R and Fiebig M 2012 Anisotropic conductance at improper ferroelectric domain walls *Nat. Mater.* **11** 284
[17] Guyonnet J, Gaponenko I, Gariglio S and Paruch P 2011 Conduction at domain walls in insulating $Pb(Zr_{0.2}Ti_{0.8})O_3$ thin films *Adv. Mater.* **23** 5377
[18] Schröder M, Haußmann A, Thiessen A, Soergel E, Woike T and Eng L M 2012 Conducting domain walls in lithium niobate single crystals *Adv. Funct. Mater.* **22** 3936
[19] Choi T, Horibe Y, Yi H T, Choi Y J, Wu W and Cheong S-W 2010 Insulating interlocked ferroelectric and structural antiphase domain walls in multiferroic $YMnO_3$ *Nat. Mater.* **9** 253
[20] Kim D J, Paudel T R, Lu H, Burton J D, Connell J G, Tsymbal E Y, Seo S S A and Gruverman A 2014 Room-temperature ferroelectricity in hexagonal $TbMnO_3$ thin films *Adv. Mater.* **26** 7660
[21] Lee J-H *et al* 2006 Epitaxial stabilization of a new multiferroic hexagonal phase of $TbMnO_3$ thin films *Adv. Mater.* **18** 3125
[22] Gruenewald J H, Nichols J and Seo S S A 2013 Pulsed laser deposition with simultaneous in situ real-time monitoring of optical spectroscopic ellipsometry and reflection high-energy electron diffraction *Rev. Sci. Instrum.* **84** 043902
[23] Bardou F 1997 Rare events in quantum tunneling *Europhys. Lett.* **39** 239
[24] Kim D J *et al* 2010 Control of defect-mediated tunneling barrier heights in ultrathin MgO films *Appl. Phys. Lett.* **97** 263502
[25] Choi W S *et al* 2008 Electronic structures of hexagonal *R*MnO_3 (*R* = Gd, Tb, Dy, and Ho) thin films: optical spectroscopy and first-principles calculations *Phys. Rev.* B **77** 045137
[26] Chiquito A J, Amorim C A, Berengue O M, Araujo L S, Bernardo E P and Leite E R 2012 Back-to-back Schottky diodes: the generalization of the diode theory in analysis and extraction of electrical parameters of nanodevices *J. Phys.: Condens. Matter* **24** 225303
[27] Jia C-L, Urban K W, Alexe M, Hesse D and Vrejoiu I 2011 Direct observation of continuous electric dipole rotation in

flux-closure domains in ferroelectric $Pb(Zr,Ti)O_3$ *Science* **331** 1420

[28] Kumagai Y and Spaldin N A 2013 Structural domain walls in polar hexagonal manganites *Nat. Commun.* **4** 1540

[29] Dawber M, Scott J F and Hartmann A J 2001 Effect of donor and acceptor dopants on Schottky barrier heights and vacancy concentrations in barium strontium titanate *J. Eur. Ceram. Soc.* **21** 1633